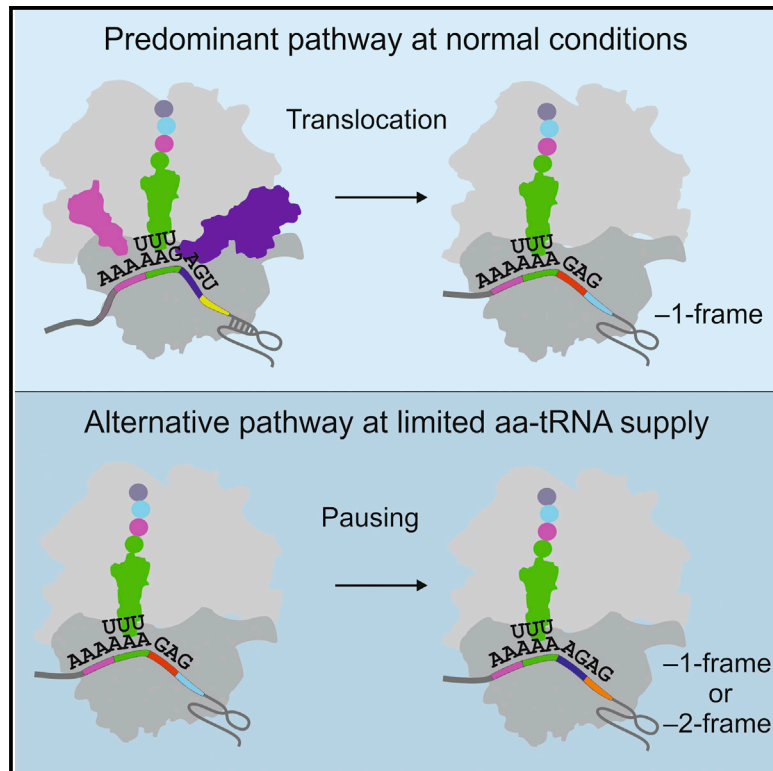


Conditional Switch between Frameshifting Regimes upon Translation of *dnaX* mRNA

Graphical Abstract



Authors

Neva Caliskan, Ingo Wohlgemuth, Natalia Korniy, Michael Pearson, Frank Peske, Marina V. Rodnina

Correspondence

rodnina@mpibpc.mpg.de

In Brief

Caliskan et al. show that ribosomes can change the reading frame depending on aminoacyl-tRNA supply. Ribosome pausing at a hungry codon leads to -1 or -2 frameshifting independent of a regulatory mRNA element normally required for programmed frameshifting. Switching between frameshifting routes can enrich coding capacity upon aminoacyl-tRNA limitation.

Highlights

- -1 frameshifting predominantly occurs upon translocation of two slippery-site tRNAs
- An alternative frameshifting pathway operates when aminoacyl-tRNA supply is limited
- Hungry frameshifting is slow and independent of the mRNA secondary structure element
- Switching between frameshifting routes can enrich coding capacity of the genome



Conditional Switch between Frameshifting Regimes upon Translation of *dnaX* mRNA

Neva Caliskan,¹ Ingo Wohlgemuth,¹ Natalia Korniy,¹ Michael Pearson,¹ Frank Peske,¹ and Marina V. Rodnina^{1,2,*}

¹Department of Physical Biochemistry, Max Planck Institute for Biophysical Chemistry, Am Fassberg 11, 37077 Göttingen, Germany

²Lead Contact

*Correspondence: rodnina@mpibpc.mpg.de

<http://dx.doi.org/10.1016/j.molcel.2017.04.023>

SUMMARY

Ribosome frameshifting during translation of bacterial *dnaX* can proceed via different routes, generating a variety of distinct polypeptides. Using kinetic experiments, we show that -1 frameshifting predominantly occurs during translocation of two tRNAs bound to the slippery sequence codons. This pathway depends on a stem-loop mRNA structure downstream of the slippery sequence and operates when aminoacyl-tRNAs are abundant. However, when aminoacyl-tRNAs are in short supply, the ribosome switches to an alternative frameshifting pathway that is independent of a stem-loop. Ribosome stalling at a vacant 0-frame A-site codon results in slippage of the P-site peptidyl-tRNA, allowing for -1 -frame decoding. When the -1 -frame aminoacyl-tRNA is lacking, the ribosomes switch into -2 frame. Quantitative mass spectrometry shows that the -2 -frame product is synthesized *in vivo*. We suggest that switching between frameshifting routes may enrich gene expression at conditions of aminoacyl-tRNA limitation.

INTRODUCTION

During the normal course of mRNA translation the ribosome initiates protein synthesis at a start codon and moves by decoding three nucleotides at a time until it reaches a stop codon where translation is terminated. Spontaneous changes of the reading frame are very rare with a frequency of about 10^{-5} per codon (Kurland, 1979; Parker, 1989). However, in some cases the mRNA guides the ribosome toward an alternative reading frame by promoting a translational slippage in the $+1$ or -1 direction (Farabaugh, 1996b; Gesteland and Atkins, 1996). Such programmed ribosome frameshifting (PRF) events are ubiquitous from viruses to mammals and operate at efficiencies from very low to as high as 80% (Tsuchihashi and Brown, 1992). PRF increases the coding capacity of genomes and regulates mRNA stability (Atkins and Gesteland, 2010; Baranov et al., 2002; Caliskan et al., 2015; Dinman, 2012; Dunkle and Dunham, 2015; Farabaugh, 1996b). In rare cases the ribosome can also shift by -2 , -4 , $+2$, $+5$, or $+6$ nucleotides (Fang et al., 2012; Lainé et al., 2008; Weiss et al., 1987; Yan et al., 2015).

-1 PRF is promoted by *cis*-acting stimulatory elements embedded in the mRNA sequence (Brakier-Gingras and Dulude, 2010; Brierley et al., 2010; Farabaugh, 1996a). The primary stimulatory element is a slippery site, usually in the form of a heptanucleotide sequence X XXY YYZ (underlined codons denote the 0 reading frame). The nucleotides in the slippery sequence (SS) allow for base pairing between the tRNA anticodon and the mRNA codon after shifting into the -1 reading frame. Another element is a stimulatory structure in the mRNA, such as a stem-loop (SL) or a pseudoknot located downstream of the SS. The mRNA secondary structure slows down translation and leads to ribosome pausing at the frameshifting site. However, the duration and the extent of the pause do not directly correlate with the efficiency of frameshifting (Kontos et al., 2001; Ritchie et al., 2012; Somogyi et al., 1993). Prokaryotic frameshifting sites may contain an additional stimulatory element, an internal Shine-Dalgarno (SD)-like sequence upstream of the SS (Larsen et al., 1994).

There are several models for -1 PRF in different systems and a number of suggested alternative pathways that may lead to -1 PRF (Baranov et al., 2004; Brierley et al., 2010; Farabaugh, 1996b; Liao et al., 2011). Our work with the model mRNA coding for the infectious bronchitis virus (IBV) proteins 1a/1b suggested that -1 PRF occurs predominantly during tRNA-mRNA translocation when the two slippery codons together with tRNAs move from the A and P to the P and E sites, respectively (Caliskan et al., 2014). The ribosome slips into the -1 frame when the head of the small ribosomal subunit (SSU) moves backward, probably because the stimulatory mRNA pseudoknot hinders the relaxation of the SSU head from the swiveled into the classical conformation. The dissociation of the E-site tRNA is delayed, and the overall residence time of EF-G on the ribosome is increased (Caliskan et al., 2014). A similar mechanism of -1 PRF was suggested for the bacterial *dnaX* gene (Chen et al., 2013, 2014; Kim et al., 2014; Yan et al., 2015). Frameshifting on *dnaX* mRNA occurs on the sequence A₁ AAA₄ AAG₇ (numbers denote the nucleotides within the SS), which is decoded by two lysine tRNAs (Blinkowa and Walker, 1990). Frameshifting is regulated by two mRNA elements, an SL structure downstream and an SD-like sequence upstream of the SS (Larsen et al., 1994). The efficiency of -1 PRF on the native *dnaX* sequence is close to 80% (Chen et al., 2014; Kim et al., 2014; Tsuchihashi and Brown, 1992). Surprisingly, frameshifting on *dnaX* can also give rise to a number of unconventional products, such as -4 or $+2$, which may result from wide-range ribosome excursions along the mRNA or from alternative pathways, in particular when the slippery sequence is mutated (Yan et al., 2015). Alternative

mechanisms for -1 PRF on *dnaX* may include different kinetic branch points and slippage during multiple attempts of tRNA binding to the A site (Chen et al., 2014); however, the latter pathway was not observed by others (Chen et al., 2013; Kim et al., 2014; Yan et al., 2015).

The apparent multitude of accessible pathways for frameshifting on *dnaX* has prompted us to explore the exact timing of slippage and the predominant kinetic route for -1 PRF using the codon-walk approach (Caliskan et al., 2014). This approach uses chemical kinetics and allows us to determine translation rates for each codon along the mRNA and to identify the branch point leading to alternative reading frame. We show that the predominant pathway for -1 PRF is identical on *dnaX* and IBV *1a/1b* mRNAs (Caliskan et al., 2014; Kim et al., 2014; Yan et al., 2015). However, we also find an alternative route that is triggered by aminoacyl-tRNA (aa-tRNA) limitation and leads to either -1 or -2 frameshifting. We dissect the branch point kinetics and the role of the mRNA SL element for the two routes to -1 and -2 frameshifting and validate the existence of -2 frameshifting in vivo by quantitative mass spectrometry. The switch to the alternative frameshifting pathway, which is due to a delay in aa-tRNA delivery to the A site of the ribosome, may explain the unusual frameshifting peptides that were identified by several groups (Chen et al., 2014; Yan et al., 2015). This switch in the mechanism provides a unifying scenario for many reported cases of frameshifting (Atkinson et al., 1997; Fang et al., 2012; Gallant and Lindsley, 1998; Kolor et al., 1993; Lainé et al., 2008; Lindsley and Gallant, 1993; Olubajo and Taylor, 2005; Temperley et al., 2010; Weiss and Gallant, 1986; Yelverton et al., 1994) and suggests yet another potential mechanism to alter the proteome composition.

RESULTS

-1 PRF Efficiency In Vitro

The *dnaX* frameshifting mRNA construct (Figure 1A) was designed in such a way that translation started at the AUG initiation codon two codons upstream of the frameshifting sequence, A₁ AAA₄ AAG₇. The SD sequence 5 nucleotides upstream of the start codon can function in translation initiation and serve as a frameshifting stimulatory signal (Kim et al., 2014). A non-essential AGU codon (Ser) downstream of the slippery codons was replaced with UUC (Phe) to simplify product analysis. Sequence and position of the SL element were as in the native *dnaX* gene (Tsuchihashi and Brown, 1992). The expected translation products in the 0 frame are fMetAla (MA), fMetAlaLys (MAK), fMetAlaLysLys (MAKK), and fMetAlaLysLysPhe (MAKKF). -1 PRF results in fMetAlaLysLysVal (MAKKV) regardless of the branch point for frameshifting. The in vitro translation system was reconstituted from *Escherichia coli* purified components, including Ala-tRNA^{Ala} (denoted as A in Figure 1), Lys-tRNA^{Lys} (K), Phe-tRNA^{Phe} (F), Val-tRNA^{Val} (V), Arg-tRNA^{Arg} (R), Glu-tRNA^{Glu} (E), and Ser-tRNA^{Ser} (S) as indicated (STAR Methods). Translation was initiated by mixing 70S initiation complexes carrying [³H]Met-tRNA^{Met} in the P site with excess ternary complexes EF-Tu-GTP-aa-tRNA and EF-G with GTP; notably, the amounts of ternary complexes were optimized to allow for the maximum translation speed and efficiency (Caliskan et al., 2014). Translation products were separated by reversed-phase

high-performance liquid chromatography (RP-HPLC) (Figure 1B), and the peak positions were identified using radioactive-labeled [³H]M and [¹⁴C]-K, -F, or -V. The double-label radioactivity assignment of the product peaks was repeated for each new product, i.e., when R, E, or S were incorporated.

We first determined the efficiency of -1 PRF from the ratio of MAKK, MAKKF, and MAKKV peptides at the end point of translation when tRNAs for A, K, F, and V were added as indicated (Figures 1C and 1D). The efficiency of -1 PRF on the mRNA containing all three stimulatory elements, SS, SL, and SD (SS/SL; SD is present in all mRNA constructs used), is about 70%, consistent with previous results obtained in vitro and in vivo (Blinkowa and Walker, 1990; Larsen et al., 1994; Tsuchihashi and Brown, 1992).

Omission of tRNAs for V or F does not affect the frameshifting efficiency (Figure 1C). The lack of interference between V and F at the A site suggests that ribosomes changed the frame before the F (UUC) or V (GUU) codons became available for decoding. With the control mRNA lacking the SS and the stimulatory SL ($-/-$), the major translation product is MAKKF in the 0 frame (93%). Also in the presence of SS alone (SS/ $-$) or SL alone ($-/SL$), the predominant product is the 0 frame MAKKF, with little amounts (5%–20%) of the -1 frame MAKKV (Figure 1D).

Branch Point for -1 PRF

To identify the kinetic branch point at which the ribosome switches from the 0 to the -1 frame, we determined the rates of amino acid incorporation during translation of *dnaX*. We expected that partitioning between the frames should change the observed rate of synthesis and signify the step at which frameshifting occurs (Liao et al., 2011). In the absence of -1 PRF, the incorporation of K and F in 0 frame is rapid (about 2.0 s⁻¹) and the formation of the -1 frame peptide negligible (Figure 1E, Table S1). When all stimulatory elements are present, the rates of K incorporation on slippery codons AAA₄ and AAG₇ (K1 and K2, respectively) do not change appreciably (Figure 1F, Table S1). In contrast, the incorporation of F is delayed, suggesting that ribosomes are stalled after K incorporation at codon K2, i.e., during or after translocation of MAKK-tRNA^{Lys} from the A to the P site. -1 frame V is incorporated very efficiently; the -1 PRF efficiency calculated from the ratio of the rate constants of V and F incorporation is 80%, consistent with the end-point measurements. The rate of codon K2 translation is slightly reduced in the presence of SL without SS, but the effect is not related to frameshifting. Ribosome stalling is due to the presence of the SL element, which delays F incorporation even in the absence of SS when there is no frameshifting (Figure 1G, Table S1). The SS alone is sufficient to induce some -1 PRF; the rates of K and F incorporation are as high as during 0-frame translation, but V incorporation is much more efficient, compared to the incorporation in the absence of SS and SL (Figure 1H).

The similarity of K incorporation kinetics, the stalling effect of SL, together with the observation that the ribosome switches the reading frame before presenting the codons for V or F in the A site (Figure 1C), suggest that the slippage occurs after the incorporation of the second K and during the translocation of the slippery codons AAA₄ AAG₇ together with the two tRNA^{Lys} molecules from the P and A to the E and P sites, respectively. This mechanism is consistent with the experimental data

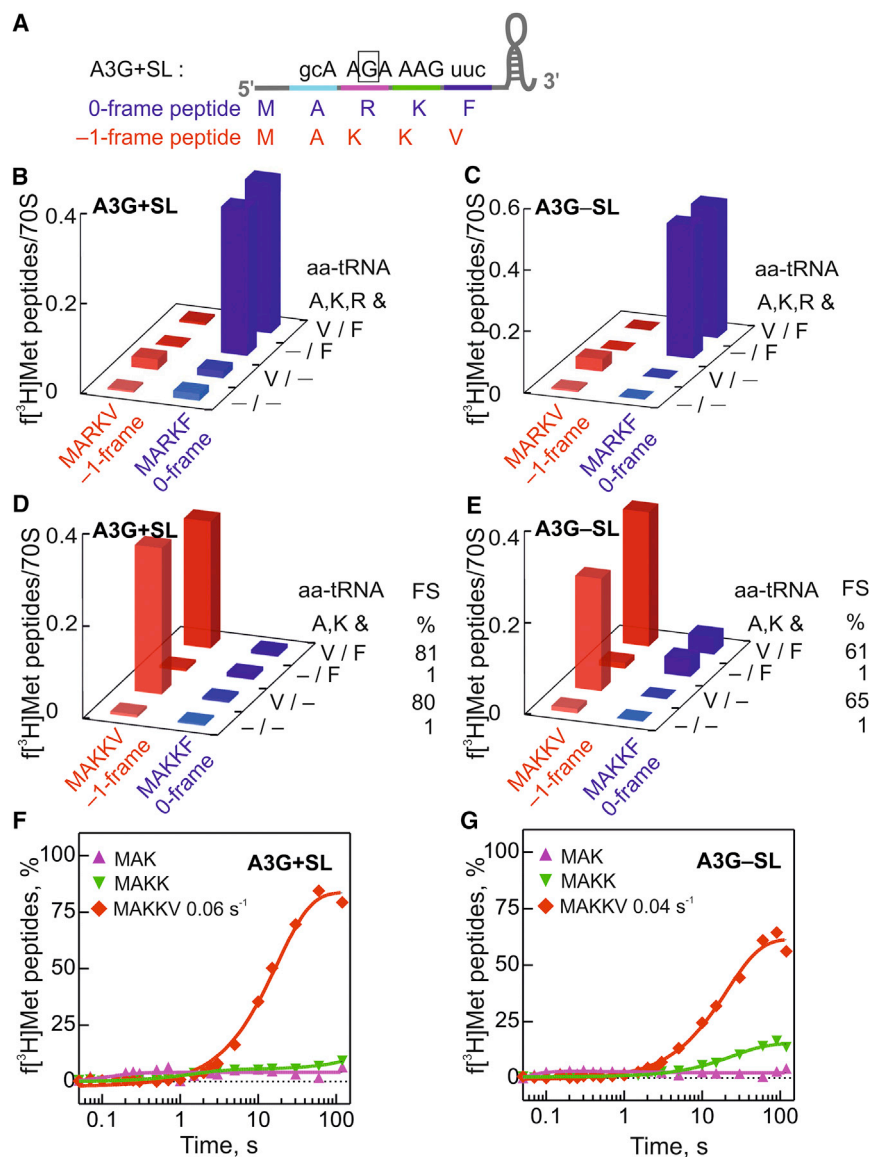


Figure 2. Translation of the A3G mRNA Slippery Site Variant

(A) Schematic of the A3G+SL mRNA used in the study. A3G mRNA variants have a point mutation at the second position of the first slippery codon from AAA₄ (K1) to AGA₄ (R), as indicated by a box. Peptides resulting from translation in 0 (MARKF) and -1 (MAKKV) reading frames are indicated.

(B and C) Amino acid incorporation in -1 (MARKV) and 0 frame (MARKF) on A3G+SL (B) and A3G-SL (C) complexes monitored at translation end points (2 min) in the presence and absence of Val-tRNA^{Val} and Phe-tRNA^{Phe} decoding the -1 and 0 frame, respectively.

(D) Same as (B) in the absence of cognate Arg-tRNA^{Arg} (R) for the AGA₄ codon.

(E) Same as (C) in the absence of cognate Arg-tRNA^{Arg} (R) for the AGA₄ codon.

(F) Codon walk over the frameshifting site of A3G+SL mRNA in the absence of Arg-tRNA^{Arg}. Eluted peptides are MAK (pink), MAKK (green), and MAKKV (red).

(G) Same as (F), but with A3G-SL mRNA. See also Figures S1 and S2 and Table S2.

of mutational analysis, which indicated that tRNA^{Lys} at both A and P sites is essential for *dnaX* frameshifting (Tsuchihashi and Brown, 1992). Again, we do not observe any of the potential alternative -4 or +2 peptides. However, when Arg-tRNA^{Arg} is omitted, the -1-frame peptide MAKKV is synthesized on both A3G and A6G mRNAs (Figures 2D and 3D). Notably, in contrast to -1PRF on the native *dnaX* sequence, synthesis of the -1-frame MAKKV peptide from the A3G and A6G variants is independent of the SL (Figures 2C-2E and 3C-3E).

In principle, incorporation of K on the AGA₄ and AGG₇ codons in the absence of R may be due to misreading, rather than frameshifting. Misreading of the R codon of A3G mRNA by Lys-tRNA^{Lys} should result in 0-frame MAKKF, and indeed we identified small amounts of that peptide in the absence of the SL (Figure 2E). The extent of misreading of the R codon by Lys-tRNA^{Lys} is also seen as a small portion of MAKK peptide that is

not converted to MAKKV in the absence of Phe-tRNA^{Phe} (Figure 2G); however, in both cases the efficiency of misreading is small compared to the extent of MAKKV formation. Similarly, on the A6G mRNA, misreading of the R codon by Lys-tRNA^{Lys} is very low, as judged from the low efficiency of 0-frame F incorporation (Figures 3B and 3C). An alternative scenario with a misreading event followed by -1 frameshifting is also unlikely (see below, Figure 4).

In the absence of significant misreading of the AGA and AGG codons, the formation of the MAK peptide on the A3G construct must be due to the reading of the -1-frame codon A₁AG by Lys-tRNA^{Lys} in the absence of the 0-frame cognate Arg-tRNA^{Arg}. Upon frameshifting, the P-site tRNA^{Ala} loses two of its 0-frame interactions with the codon, which changes from GCA to GGC. On A6G, -1 frameshifting re-establishes a cognate codon-anticodon interaction in the P site. Because this frameshifting route is operational in the absence of the cognate 0-frame tRNA and is not “programmed” by an SL element, we denote it as the aa-tRNA depletion-stimulated frameshifting (ADF) pathway.

The kinetics of ADF is quite distinct from that of conventional -1PRF. The rate of V incorporation on A3G is about 0.05 s⁻¹ (Figures 2F, 2G, and S3; Table S2), i.e., much slower than on the native sequence with all cognate aa-tRNAs present (compare to SS/SL mRNA; Figure 1F). Upon A3G translation, MAK or MAKK peptides do not accumulate (Figure 2F), indicating that, as soon as K is incorporated as a result of -1 frameshifting, the following codons are rapidly translated leading to the MAKKV

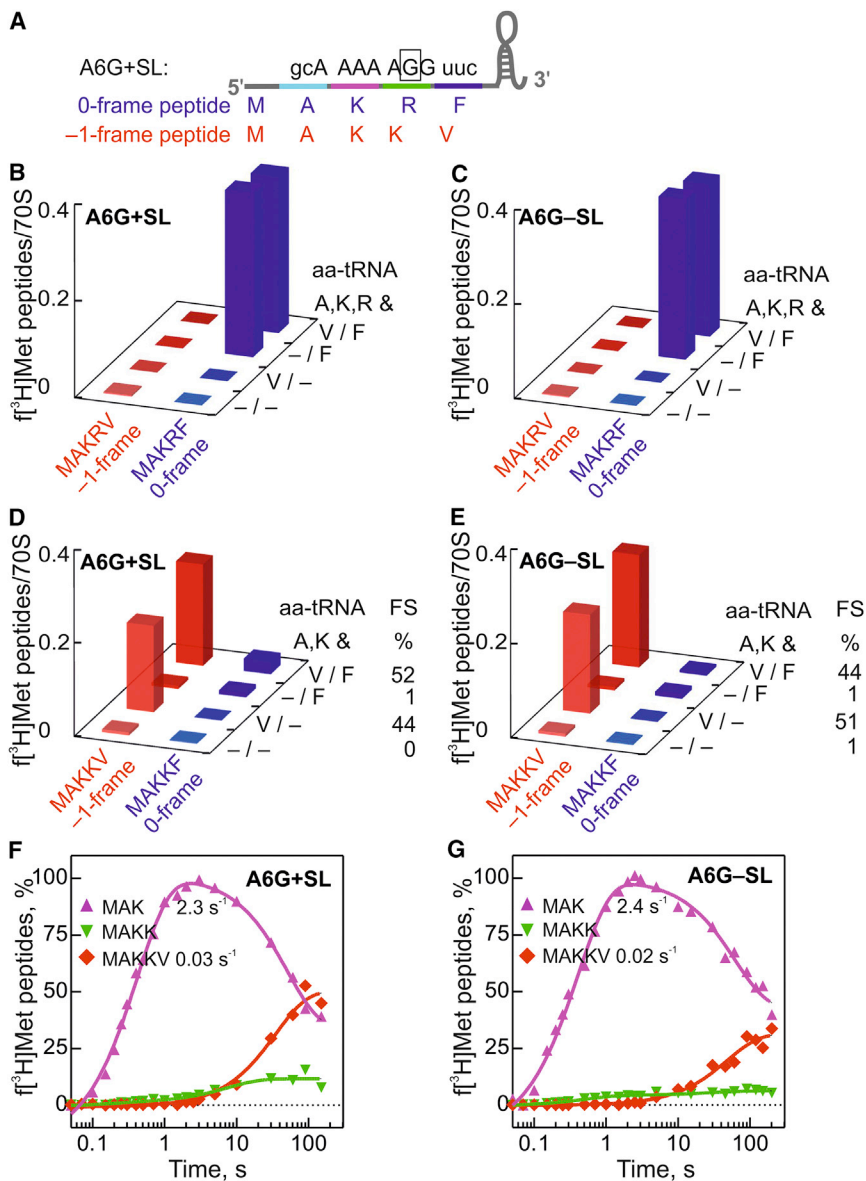


Figure 3. Translation of A6G mRNA Slippery Site Variants

(A) Schematic of the A6G+SL mRNA. A6G mRNA variants have a point mutation from AAG₇ (K) to AGG₇ (R), indicated by the box. Peptides translated in 0 (MAKRF) and -1 (MAKKV) reading frame are indicated.

(B and C) Amino acid incorporation in -1 and 0 frame on A6G+SL (B) and A6G-SL (C) complexes, as monitored at translation end points (2 min).

(D) Same as (B) in the absence of cognate Arg-tRNA^{Arg} decoding for the AGG₇ codon.

(E) Same as (C) in the absence of cognate Arg-tRNA^{Arg} decoding for the AGG₇ codon.

(F) The codon walk over the frameshifting site of A6G+SL mRNA in the absence of Arg-tRNA^{Arg}. Monitored peptides are MAK (pink), MAKK (green), and MAKKV (red).

(G) Same as (F), but with A6G-SL mRNA.

See also Figures S1 and S2 and Table S2.

peptide. This implies that the apparent rate constant of V incorporation in fact represents the rate of MAK synthesis, which is almost 30-fold lower than on the SS/SL construct (Tables S1 and S2). With the A6G variant, the formation of the MAK peptide in the absence of R is rapid (1.4 s^{-1}) (Figures 3D and 3E), as expected for undisturbed K incorporation (Table S1). The MAK peptide accumulates because now the rate-limiting step is the incorporation of the second K upon -1 frameshifting on the A₄ AGG₇ sequence. MAKKV is synthesized as soon as MAKK has been made, which explains why MAKK does not accumulate (Figures 3F and 3G). Thus, the apparent rate constant of MAKKV synthesis, about 0.02 s^{-1} , reflects the rate-limiting step of MAKK formation as a result of ADF on A₄ AGG₇.

The A6G sequence A₁ AAA₄ AGG₇ offers multiple potential scenarios for tRNA slippage, e.g., during translocation of K1 or binding of K2. To clarify the branch point of frameshifting and

whether it depends on tRNA^{Lys} as A-site substrate, we have generated an A4GA6G mRNA variant with the sequence A₁ AAG₄ AGG₇. The slippery site limits tRNA^{Lys} slippage to codon K1 (A₁ AAG₄) and encodes MAKRF in 0 frame versus MAKEV in -1 frame (Figure 4A). In the presence of all cognate 0-frame aa-tRNA substrates (A, K, R, and F), only the 0-frame peptide is synthesized (Figure 4B). In the absence of Arg-tRNA^{Arg}, which is the 0-frame-cognate substrate for codon II, the major product is the -1-frame MAKEV (36%) (Figure 4C). In the absence of both Arg-tRNA^{Arg} and Glu-tRNA^{Glu}, peptides are translated up to MAK and no -1-frame product is observed (Figure 4C), suggesting that misreading of the AGG codon in the 0 frame is negligible. Also the scenario in which Lys-tRNA^{Lys} misreads the AGG

codon and then slips into the -1 frame is excluded, as this would result in an MAKKV peptide, which was not detected. The MAK peptide is synthesized rapidly and accumulates as with the A6G variant (Figure 4D). The formation of the -1-frame MAKEV is slow (0.014 s^{-1}) and represents an ADF event preceding the E incorporation step (Figure 4D). Also in this case F (0 frame) and V (-1 frame) tRNAs do not compete, suggesting that partitioning between the reading frames has occurred prior to F and V decoding (Figures 4B and 4C).

Taken together, the results obtained with A3G, A6G, and A4GA6G mRNAs demonstrate that the P-site peptidyl-tRNA^{Lys} can slip into the -1 frame when the A site is vacant. This ADF pathway requires only a slippery tetranucleotide sequence (A AAA or A AAG), does not require the SL stimulator, and is slow compared to the predominant -1 frameshifting. The ADF route crucially depends on a hungry codon in the A site. In the

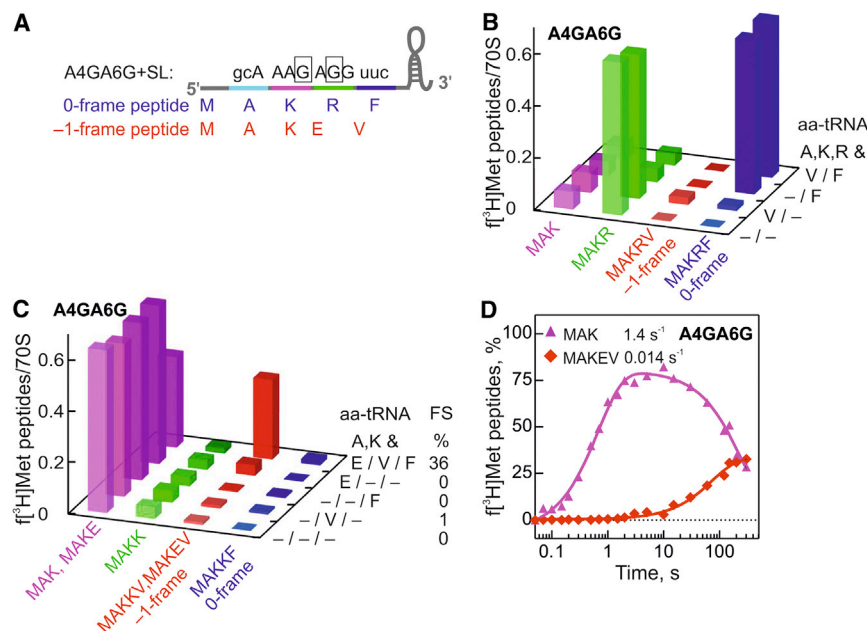


Figure 4. Translation of the Slippery Site Variant A4GA6G mRNA

(A) Schematic of the A4GA6G mRNA. (B) Amino acid incorporation in -1 and 0 frame monitored at translation end point (2 min) in the absence of -1-frame Glu-tRNA^{Glu}. (C) Same as (B) in the absence of the 0-frame Arg-tRNA^{Arg} and in the presence of -1-frame Glu-tRNA^{Glu}. (D) Codon walk in the absence of Arg-tRNA^{Arg}. Monitored peptides are MAK (pink) and MAKEV (red). See also Figure S2 and Table S2.

DISCUSSION

Predominant Pathway to -1PRF

The data presented here show how two different pathways can lead to frameshifting during translation of *dnaX* mRNA (Figure 6). In the predominant pathway, which operates at conditions of efficient translation, the branch point for -1PRF is during

presence of the cognate aa-tRNA, the pathway does not operate and translation proceeds in the 0 frame without a pause (Figures S1 and S2).

-2 Frameshifting on the A AAA AAG Sequence

Next, we asked what happens on the native *dnaX* sequence when the -1-frame tRNA^{Val} is omitted. In addition to tRNAs for A, K, V, and F required for 0 and -1 frames (as well as for -4 and +2 frames), we added Ser-tRNA^{Ser} reading the -2-frame AGU codon (Figure 5A). When all aa-tRNAs are present, S is not incorporated into peptides and, as expected, only MAKKV and MAKKF peptides are synthesized (Figure 5B). However, in the absence of Val-tRNA^{Val}, about 20% of peptides incorporate S to form the MAKKS peptide; F incorporation into the 0-frame MAKKF is not affected. -2-frame translation is slow compared to the -1PRF route operating at aa-tRNA saturation and required both the slippery sequence and the mRNA regulatory element (Figures 5C and 5D, Table S1). These results indicate that the ribosomes can undergo a double slippage: the first branch point is at codon K2 during translocation of MAKK-tRNA^{Lys} from the A to the P site, where the ribosomes partition between 0 and -1 frame. If both Val- and Phe-tRNAs are present, they rapidly read their respective codons, thereby committing the ribosome for further synthesis in the respective frame. However, if Val-tRNA^{Val} is absent, MAKK-tRNA^{Lys}, which now binds to the -1-frame codon in the P site, can slip further into the -2 frame, allowing for binding of Ser-tRNA^{Ser}, which is cognate to the codon in the A site. We envisage that such a mechanism—when applied to translation of longer sequences at conditions of aa-tRNA limitations—can result in a multitude of different frameshifting peptides.

To test the existence of the -2 frameshifting product in vivo, we quantified it in *E. coli* lysates using mass spectrometry (Figure S3, Table S3). The yield of -2-frame product relative to -1-frame product is ~0.5%. Thus, -2 frameshifting can occur in vivo.

translocation at slippery codon 2. This pathway was suggested for *dnaX* based on single-molecule FRET and optical tweezers experiments (Kim et al., 2014; Yan et al., 2015) and for IBV *1a/1b* by real-time kinetic analysis of peptides synthesized in the 0 and -1 frames (Caliskan et al., 2014). Furthermore, the peptide analysis of the translation products of the human immunodeficiency virus type 1 (HIV-1) *gag-pol* fragment suggested that this mechanism is likely to operate also in that case (Jacks et al., 1988; Yelverton et al., 1994). In contrast to *dnaX*, which has a SS coding for K in both 0 and -1 frames regardless of the exact branch point, -1PRF on HIV mRNA alters the peptide sequence in a different way depending on the exact point of slippage. This simplifies the identification of the frameshifting branch point by peptide analysis. The product of -1-frame translation contains the amino acid encoded by the 0-frame codon 2 of the slippery sequence (Jacks et al., 1988; Yelverton et al., 1994), indicating that frameshifting occurs after translation of codon 2 (Yelverton et al., 1994). A characteristic feature of this route in *dnaX*, IBV, or HIV-1 is that it is facilitated by the mRNA stimulatory element downstream of the SS and does not depend on the competition between aa-tRNAs reading the 0- and -1-frame codons downstream of the slippery sequence (Caliskan et al., 2014; Gallant and Lindsley, 1993). This mechanism may cover most examples of the so-called “dual slippage,” that is when two tRNAs are bound to the ribosome during frameshifting (Horsfield et al., 1995; Jacks et al., 1988; Kim et al., 2014; Yan et al., 2015; Yelverton et al., 1994).

From the mechanistic point of view, translocation-dependent -1PRF occurs at the structural barrier presented by the mRNA element, SL or pseudoknot, which causes the ribosome to stall and undergo multiple translocation attempts (Caliskan et al., 2014; Chen et al., 2014; Kim et al., 2014; Namy et al., 2006; Yan et al., 2015). While details of the mechanism remain to be shown for frameshifting on *dnaX*, HIV-1, and other frameshifting sequences, frameshifting on IBV occurs when the tRNAs have

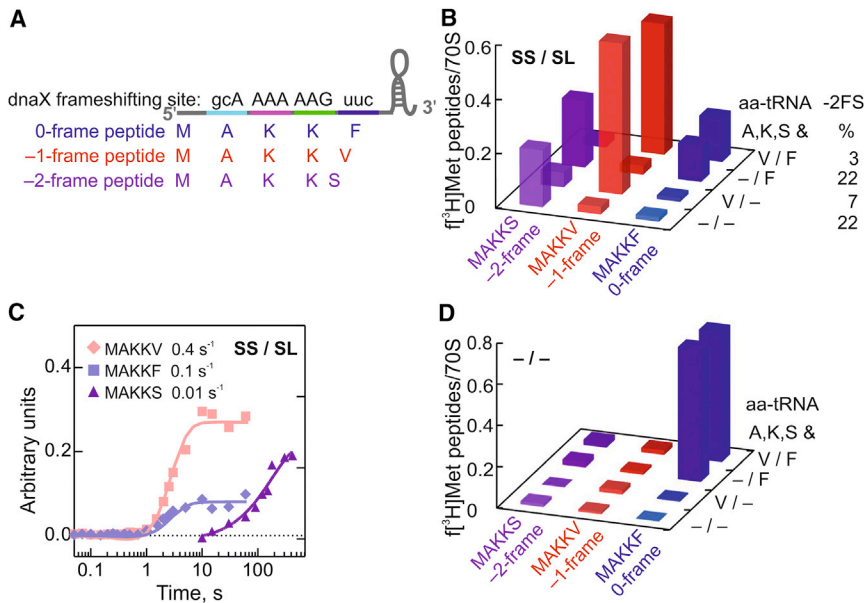


Figure 5. -2 Frameshifting on *dnaX*

(A) Schematic of the *dnaX* mRNA (SS/SL) and peptides translated in 0, -1, and -2 reading frame. (B) S incorporation upon omission of Val-tRNA^{Val}. (C) Comparison of the rate constants of F, V, and S incorporation on SS/SL mRNA in 0, -1, and -2 reading frame. Time courses of F and V incorporation are taken from Figure 1D for comparison. (D) Same as (B), but with the (-/-) mRNA. See also Figure S3 and Table S3.

already moved from the A to P and P to E sites, respectively, and the E-site tRNA most probably lost its codon-anticodon interaction, thereby limiting the base pairing to the P-site tRNA only (Caliskan et al., 2014; Chen et al., 2013). Dissociation of the E-site tRNA and backward swiveling motion of the SSU head are delayed due to the presence of the mRNA secondary structure element (Caliskan et al., 2014; Chen et al., 2013, 2014; Kim et al., 2014). The block of translation is resolved upon ribosome slippage into the -1 frame. EF-G requires multiple attempts to complete translocation, which in effect appears as if it remained bound to the ribosome (Chen et al., 2014; Namy et al., 2006).

Alternative Frameshifting Pathway

When the tRNA cognate to the slippery codon is missing and the A site remains vacant, the ribosome may switch to an alternative route of frameshifting on *dnaX* (Figure 6). The idling ribosome makes excursions along the mRNA outside the 0 frame; apparently P-site codon-anticodon interactions are destabilized or do not prevent the ribosome from sliding along the mRNA, similarly to what is observed during ribosome bypassing (Samatova et al., 2014). As soon as the ribosome arrives at a codon for which an aa-tRNA is available, regular decoding takes place and translation can resume. This type of frameshifting is independent of the SL element in the mRNA, can occur at any slippery codon, but is much slower than -1PRF taking place during translocation. The slippage of the idling ribosome waiting for the A-site aa-tRNA may explain the appearance of peptide products from a variety of alternative reading frames, such as -2 frame (this paper) or -4 and +2 frames (Yan et al., 2015). In the latter case, the in vitro translation system used to accumulate the peptides for mass spectrometry and to perform optical tweezers experiments may over time become depleted of some aa-tRNAs, which may facilitate ribosome pausing and excursions into alternative frames. Characteristically, frameshifting at a hungry codon correlates with a large amount of incomplete peptides

(Yelverton et al., 1994), which is consistent with the presence of incomplete translation products of in vitro *dnaX* translation (Yan et al., 2015). Similarly, the imbalance of the in vitro translation pool may be the reason for the observed frameshifting branch point at the SS codon K1 by Chen et al., who observed unusual multiple unsuccessful decoding attempts of Lys-tRNA^{Lys}, and a large portion of ribosomes stalled on slippery codons K1 and K2 (Chen et al., 2014), in contrast to the results of the present work or of Kim et al. (2014). In our example of a hungry codon-stimulated -2 frameshifting, the new reading frame is entered by double slippage: the ribosomes first undergo an SL-dependent -1PRF, which is followed by a further slippage into the -2 frame when the aa-tRNA decoding the -1 frame is missing.

aa-tRNA Depletion and Frameshifting In Vivo

Hungry codons are known to affect frameshifting in vivo (Atkinson et al., 1997; Gallant and Lindsley, 1992; Gurvich et al., 2005; Olubajo and Taylor, 2005; Temperley et al., 2010; Yelverton et al., 1994). In particular, the limitation for Lys-tRNA^{Lys} (for AAA and AAG codons) and Arg-tRNA^{Arg} (for AGA and AGG codons) stimulates frameshifting (Barak et al., 1996b; Lainé et al., 2008; Spanjaard et al., 1990). For HIV-1 *gag-pol*, this route may account for -1-frame peptides that have been observed in vivo using reporter systems and in vitro upon translation in cell extracts (Cardno et al., 2015; Jacks et al., 1988; Lin et al., 2012; Yelverton et al., 1994). We note that both in vivo and in vitro aa-tRNA pools are likely to be imbalanced due to protein overexpression and potentially limiting amounts of aa-tRNAs, respectively. The frequency of frameshifting is strongly influenced by the identity of the mRNA nucleotides at positions two, three, and four upstream of the actual frameshifting site and appears to depend on the possibilities of base-pairing between the coding sequence and the anticodon of the P-site peptidyl-tRNA when shifted by one nucleotide (Barak et al., 1996b; Kolor et al., 1993), although cases with no or only one P-site codon-anticodon interaction have also been reported (Licznar et al., 2003). We observe efficient frameshifting with P-site peptidyl-tRNA^{Ala}, which has only a single-position match to the -1-frame codon; the mechanism of this unusual recoding event remains to be investigated. Frameshifting mediated by low aa-tRNA abundance may also explain other cases of single-tRNA slippage events (Baranov et al., 2004 and references cited therein).

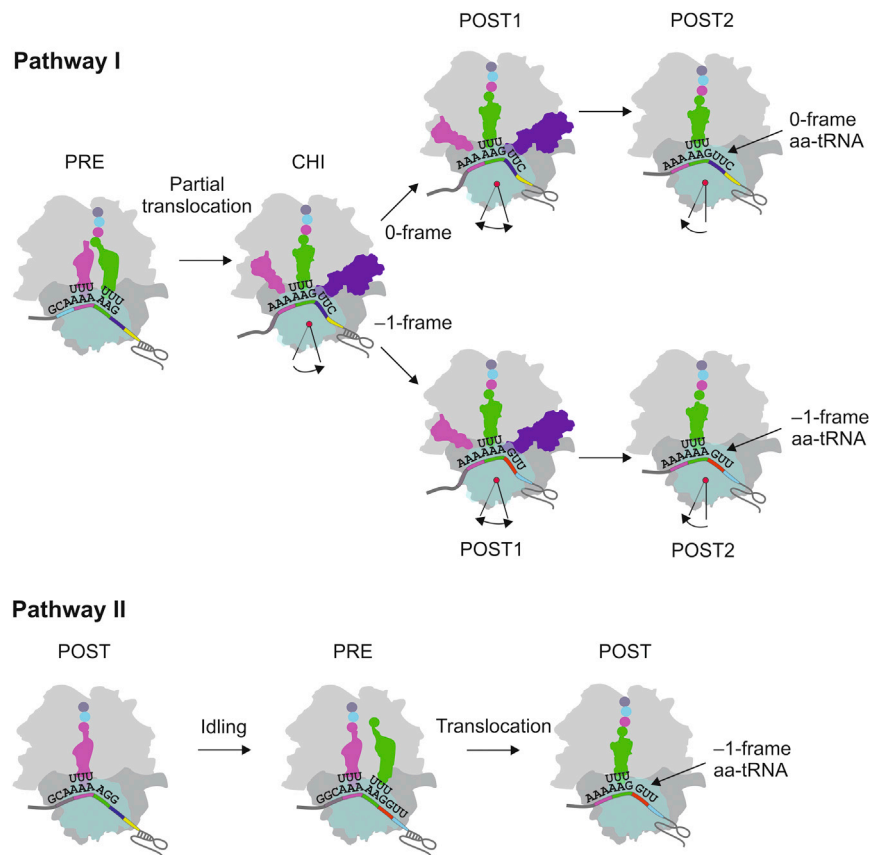


Figure 6. Models of Alternative Frameshifting Mechanisms

(A) -1 PRF during translocation.
 (B) Frameshifting induced by ribosome stalling due to limitation of aa-tRNA cognate to the A-site codon (ADF).

There are several further examples which can be explained by ADF *in vivo*. Rare arginine codons, AGG and AGA, cause significant levels of -1 frameshifting and premature termination of translation of human mitochondrial mRNAs (Temperley et al., 2010). When mammalian antizyme is expressed artificially in budding yeast, the full-length antizyme product is expressed via -2 frameshifting, which is thought to involve mainly P-site slippage with an empty A site (Ivanov et al., 1998; Matsufuji et al., 1996). Porcine reproductive and respiratory syndrome virus (PRRSV) uses -1 and -2 frameshifting at a conserved G GUU UUU sequence (Fang et al., 2012). Because in some members of the PRRSV family -1 frameshifting brings a stop codon into the A site, which should result in termination, it is tempting to speculate that termination is slow and -2 frameshifting results from slippage of ribosomes with empty A site. Like in the HIV-1 *gag-pol* gene, -1 frameshifting in the HIV-1 *env* gene is enhanced by a hungry codon mechanism (Olubajo and Taylor, 2005); equine infectious anemia virus (EIAV), a retrovirus related to HIV-1, may employ a similar mechanism (Lin et al., 2016). Frameshifting increases in stationary phase cells, which may be explained by aa-tRNA limitation (Barak et al., 1996a). We suggest that ribosomes can employ different frameshifting pathways on the same slippery sequence, switching from PRF to ADF and extending the repertoire of accessible reading frames under certain cellular conditions such as starvation or infection (Lainé et al., 2008; Olubajo and Taylor, 2005). Changing the reading frame through the availability of aa-tRNAs

may provide an efficient way to modulate the cellular proteome to adjust to the cellular environment and to achieve alternative gene expression.

STAR★METHODS

Detailed methods are provided in the online version of this paper and include the following:

- KEY RESOURCES TABLE
- CONTACT FOR REAGENT AND RESOURCE SHARING
- METHOD DETAILS
 - Introducing a FLAG tag
 - mRNA constructs
 - tRNA preparation
 - Translation assays
 - Mass Spectrometry

SUPPLEMENTAL INFORMATION

Supplemental Information includes three figures and four tables and can be found with this article online at <http://dx.doi.org/10.1016/j.molcel.2017.04.023>.

AUTHOR CONTRIBUTIONS

All authors conceived the research and designed experiments, N.C. performed most of the experiments and analyzed the data; I.W. performed mass

spectrometry experiments; N.C., N.K., and M.P. prepared materials; N.C. and M.V.R. wrote the paper with contributions of all authors.

ACKNOWLEDGMENTS

We thank Wolfgang Wintermeyer for the suggestions on the manuscript and Anna Bursy, Olaf Geintzer, Sandra Kappler, Christina Kothe, Monika Raabe, Theresia Uhlendorf, Tanja Wiles, and Michael Zimmermann for expert technical assistance. We thank Henning Urlaub and the group of Bioanalytical Mass Spectrometry for mass spectrometry analysis. The work was supported by grants of the Deutsche Forschungsgemeinschaft (SFB860 for M.V.R. and FOR1805 for I.W. and M.V.R.). N.K. was supported by the fellowship of the Boehringer Ingelheim Foundation.

Received: July 26, 2016

Revised: March 7, 2017

Accepted: April 27, 2017

Published: May 18, 2017

REFERENCES

- Atkins, J., and Gesteland, R.F. (2010). Recoding: expansion of decoding rules enriches gene expression (Springer).
- Atkinson, J., Dodge, M., and Gallant, J. (1997). Secondary structures and starvation-induced frameshifting. *Mol. Microbiol.* **26**, 747–753.
- Barak, Z., Gallant, J., Lindsley, D., Kwieciszewski, B., and Heidele, D. (1996a). Enhanced ribosome frameshifting in stationary phase cells. *J. Mol. Biol.* **263**, 140–148.
- Barak, Z., Lindsley, D., and Gallant, J. (1996b). On the mechanism of leftward frameshifting at several hungry codons. *J. Mol. Biol.* **256**, 676–684.
- Baranov, P.V., Gesteland, R.F., and Atkins, J.F. (2002). Recoding: translational bifurcations in gene expression. *Gene* **286**, 187–201.
- Baranov, P.V., Gesteland, R.F., and Atkins, J.F. (2004). P-site tRNA is a crucial initiator of ribosomal frameshifting. *RNA* **10**, 221–230.
- Blinkowa, A.L., and Walker, J.R. (1990). Programmed ribosomal frameshifting generates the Escherichia coli DNA polymerase III gamma subunit from within the tau subunit reading frame. *Nucleic Acids Res.* **18**, 1725–1729.
- Brakier-Gingras, L., and Dulude, D. (2010). Programmed –1 ribosomal frameshift in the human immunodeficiency virus of type 1. In *Recoding: Expansion of Decoding Rules Enriches Gene Expression* (Springer), pp. 175–192.
- Brierley, I., Gilbert, R.J.C., and Pennell, S. (2010). Pseudoknot-Dependent Programmed-1 Ribosomal Frameshifting: Structures, Mechanisms and Models. In *Recoding: Expansion of Decoding Rules Enriches Gene Expression* (Springer), pp. 149–174.
- Caliskan, N., Katunin, V.I., Belardinelli, R., Peske, F., and Rodnina, M.V. (2014). Programmed -1 frameshifting by kinetic partitioning during impeded translocation. *Cell* **157**, 1619–1631.
- Caliskan, N., Peske, F., and Rodnina, M.V. (2015). Changed in translation: mRNA recoding by -1 programmed ribosomal frameshifting. *Trends Biochem. Sci.* **40**, 265–274.
- Cardno, T.S., Shimaki, Y., Sleebs, B.E., Lackovic, K., Parisot, J.P., Moss, R.M., Crowe-McAuliffe, C., Mathew, S.F., Edgar, C.D., Kleffmann, T., and Tate, W.P. (2015). HIV-1 and Human PEG10 Frameshift Elements Are Functionally Distinct and Distinguished by Novel Small Molecule Modulators. *PLoS ONE* **10**, e0139036.
- Chen, C., Zhang, H., Broitman, S.L., Reiche, M., Farrell, I., Cooperman, B.S., and Goldman, Y.E. (2013). Dynamics of translation by single ribosomes through mRNA secondary structures. *Nat. Struct. Mol. Biol.* **20**, 582–588.
- Chen, J., Petrov, A., Johansson, M., Tsai, A., O’Leary, S.E., and Puglisi, J.D. (2014). Dynamic pathways of -1 translational frameshifting. *Nature* **512**, 328–332.
- Cunha, C.E., Belardinelli, R., Peske, F., Holtkamp, W., Wintermeyer, W., and Rodnina, M.V. (2013). Dual use of GTP hydrolysis by elongation factor G on the ribosome. *Translation (Austin)* **1**, e24315.
- Dinman, J.D. (2012). Mechanisms and implications of programmed translational frameshifting. *Wiley Interdiscip. Rev. RNA* **3**, 661–673.
- Dunkle, J.A., and Dunham, C.M. (2015). Mechanisms of mRNA frame maintenance and its subversion during translation of the genetic code. *Biochimie* **114**, 90–96.
- Fang, Y., Treffers, E.E., Li, Y., Tas, A., Sun, Z., van der Meer, Y., de Ru, A.H., van Veelen, P.A., Atkins, J.F., Snijder, E.J., and Firth, A.E. (2012). Efficient -2 frameshifting by mammalian ribosomes to synthesize an additional arterivirus protein. *Proc. Natl. Acad. Sci. USA* **109**, E2920–E2928.
- Farabaugh, P.J. (1996a). Programmed translational frameshifting. *Annu. Rev. Genet.* **30**, 507–528.
- Farabaugh, P.J. (1996b). Programmed translational frameshifting. *Microbiol. Rev.* **60**, 103–134.
- Gallant, J.A., and Lindsley, D. (1992). Leftward ribosome frameshifting at a hungry codon. *J. Mol. Biol.* **223**, 31–40.
- Gallant, J., and Lindsley, D. (1993). Ribosome frameshifting at hungry codons: sequence rules, directional specificity and possible relationship to mobile element behaviour. *Biochem. Soc. Trans.* **21**, 817–821.
- Gallant, J.A., and Lindsley, D. (1998). Ribosomes can slide over and beyond “hungry” codons, resuming protein chain elongation many nucleotides downstream. *Proc. Natl. Acad. Sci. USA* **95**, 13771–13776.
- Gallien, S., Duriez, E., Crone, C., Kellmann, M., Moehring, T., and Domon, B. (2012). Targeted proteomic quantification on quadrupole-orbitrap mass spectrometer. *Mol. Cell. Proteomics* **11**, 1709–1723.
- Gesteland, R.F., and Atkins, J.F. (1996). Recoding: dynamic reprogramming of translation. *Annu. Rev. Biochem.* **65**, 741–768.
- Gibson, D.G., Young, L., Chuang, R.Y., Venter, J.C., Hutchison, C.A., 3rd, and Smith, H.O. (2009). Enzymatic assembly of DNA molecules up to several hundred kilobases. *Nat. Methods* **6**, 343–345.
- Gurvich, O.L., Baranov, P.V., Gesteland, R.F., and Atkins, J.F. (2005). Expression levels influence ribosomal frameshifting at the tandem rare arginine codons AGG_AGG and AGA_AGA in Escherichia coli. *J. Bacteriol.* **187**, 4023–4032.
- Horsfield, J.A., Wilson, D.N., Mannering, S.A., Adamski, F.M., and Tate, W.P. (1995). Prokaryotic ribosomes recode the HIV-1 gag-pol-1 frameshift sequence by an E/P site post-translocation simultaneous slippage mechanism. *Nucleic Acids Res.* **23**, 1487–1494.
- Ivanov, I.P., Gesteland, R.F., Matsufuji, S., and Atkins, J.F. (1998). Programmed frameshifting in the synthesis of mammalian antizyme is +1 in mammals, predominantly +1 in fission yeast, but -2 in budding yeast. *RNA* **4**, 1230–1238.
- Jacks, T., Madhani, H.D., Masiarz, F.R., and Varmus, H.E. (1988). Signals for ribosomal frameshifting in the Rous sarcoma virus gag-pol region. *Cell* **55**, 447–458.
- Kim, H.K., Liu, F., Fei, J., Bustamante, C., Gonzalez, R.L., Jr., and Tinoco, I., Jr. (2014). A frameshifting stimulatory stem loop destabilizes the hybrid state and impedes ribosomal translocation. *Proc. Natl. Acad. Sci. USA* **111**, 5538–5543.
- Kolor, K., Lindsley, D., and Gallant, J.A. (1993). On the role of the P-site in leftward ribosome frameshifting at a hungry codon. *J. Mol. Biol.* **230**, 1–5.
- Kontos, H., Naphine, S., and Brierley, I. (2001). Ribosomal pausing at a frameshifter RNA pseudoknot is sensitive to reading phase but shows little correlation with frameshift efficiency. *Mol. Cell. Biol.* **21**, 8657–8670.
- Kothe, U., Paleskava, A., Konevega, A.L., and Rodnina, M.V. (2006). Single-step purification of specific tRNAs by hydrophobic tagging. *Anal. Biochem.* **356**, 148–150.
- Kurland, C. (1979). Reading frame errors on ribosomes. In *Nonsense Mutations and tRNA Suppressors* (New York, NY: Academic Press), pp. 97–108.
- Lainé, S., Thouard, A., Komar, A.A., and Rossignol, J.M. (2008). Ribosome can resume the translation in both +1 or -1 frames after encountering an AGA cluster in Escherichia coli. *Gene* **412**, 95–101.

- Larsen, B., Wills, N.M., Gesteland, R.F., and Atkins, J.F. (1994). rRNA-mRNA base pairing stimulates a programmed -1 ribosomal frameshift. *J. Bacteriol.* *176*, 6842–6851.
- Liao, P.Y., Choi, Y.S., Dinman, J.D., and Lee, K.H. (2011). The many paths to frameshifting: kinetic modelling and analysis of the effects of different elongation steps on programmed -1 ribosomal frameshifting. *Nucleic Acids Res.* *39*, 300–312.
- Licznar, P., Mejlhede, N., Prère, M.F., Wills, N., Gesteland, R.F., Atkins, J.F., and Fayet, O. (2003). Programmed translational -1 frameshifting on hexanucleotide motifs and the wobble properties of tRNAs. *EMBO J.* *22*, 4770–4778.
- Lin, Z., Gilbert, R.J., and Brierley, I. (2012). Spacer-length dependence of programmed -1 or -2 ribosomal frameshifting on a U6A heptamer supports a role for messenger RNA (mRNA) tension in frameshifting. *Nucleic Acids Res.* *40*, 8674–8689.
- Lin, Y.Z., Sun, L.K., Zhu, D.T., Hu, Z., Wang, X.F., Du, C., Wang, Y.H., Wang, X.J., and Zhou, J.H. (2016). Equine schlafen 11 restricts the production of equine infectious anemia virus via a codon usage-dependent mechanism. *Virology* *495*, 112–121.
- Lindsley, D., and Gallant, J. (1993). On the directional specificity of ribosome frameshifting at a “hungry” codon. *Proc. Natl. Acad. Sci. USA* *90*, 5469–5473.
- Link, A.J., Phillips, D., and Church, G.M. (1997). Methods for generating precise deletions and insertions in the genome of wild-type *Escherichia coli*: application to open reading frame characterization. *J. Bacteriol.* *179*, 6228–6237.
- MacLean, B., Tomazela, D.M., Shulman, N., Chambers, M., Finney, G.L., Frewen, B., Kern, R., Tabb, D.L., Liebler, D.C., and MacCoss, M.J. (2010). Skyline: an open source document editor for creating and analyzing targeted proteomics experiments. *Bioinformatics* *26*, 966–968.
- Matsufuji, S., Matsufuji, T., Wills, N.M., Gesteland, R.F., and Atkins, J.F. (1996). Reading two bases twice: mammalian antizyme frameshifting in yeast. *EMBO J.* *15*, 1360–1370.
- Namy, O., Moran, S.J., Stuart, D.I., Gilbert, R.J., and Brierley, I. (2006). A mechanical explanation of RNA pseudoknot function in programmed ribosomal frameshifting. *Nature* *441*, 244–247.
- Olubajo, B., and Taylor, E.W. (2005). A -1 frameshift in the HIV-1 env gene is enhanced by arginine deficiency via a hungry codon mechanism. *Mutat. Res.* *579*, 125–132.
- Parker, J. (1989). Errors and alternatives in reading the universal genetic code. *Microbiol. Rev.* *53*, 273–298.
- Peterson, A.C., Russell, J.D., Bailey, D.J., Westphall, M.S., and Coon, J.J. (2012). Parallel reaction monitoring for high resolution and high mass accuracy quantitative, targeted proteomics. *Mol. Cell. Proteomics* *11*, 1475–1488.
- Ritchie, D.B., Foster, D.A., and Woodside, M.T. (2012). Programmed -1 frameshifting efficiency correlates with RNA pseudoknot conformational plasticity, not resistance to mechanical unfolding. *Proc. Natl. Acad. Sci. USA* *109*, 16167–16172.
- Rodnina, M.V., Savelsbergh, A., Katunin, V.I., and Wintermeyer, W. (1997). Hydrolysis of GTP by elongation factor G drives tRNA movement on the ribosome. *Nature* *385*, 37–41.
- Rodnina, M.V., Savelsbergh, A., Matassova, N.B., Katunin, V.I., Semenov, Y.P., and Wintermeyer, W. (1999). Thiostrepton inhibits the turnover but not the GTPase of elongation factor G on the ribosome. *Proc. Natl. Acad. Sci. USA* *96*, 9586–9590.
- Samatova, E., Konevega, A.L., Wills, N.M., Atkins, J.F., and Rodnina, M.V. (2014). High-efficiency translational bypassing of non-coding nucleotides specified by mRNA structure and nascent peptide. *Nat. Commun.* *5*, 4459.
- Savelsbergh, A., Katunin, V.I., Mohr, D., Peske, F., Rodnina, M.V., and Wintermeyer, W. (2003). An elongation factor G-induced ribosome rearrangement precedes tRNA-mRNA translocation. *Mol. Cell* *11*, 1517–1523.
- Shevchenko, A., Tomas, H., Havlis, J., Olsen, J.V., and Mann, M. (2006). In-gel digestion for mass spectrometric characterization of proteins and proteomes. *Nat. Protoc.* *1*, 2856–2860.
- Somogyi, P., Jenner, A.J., Brierley, I., and Inglis, S.C. (1993). Ribosomal pausing during translation of an RNA pseudoknot. *Mol. Cell. Biol.* *13*, 6931–6940.
- Spanjaard, R.A., Chen, K., Walker, J.R., and van Duin, J. (1990). Frameshift suppression at tandem AGA and AGG codons by cloned tRNA genes: assigning a codon to argU tRNA and T4 tRNA(Arg). *Nucleic Acids Res.* *18*, 5031–5036.
- Temperley, R., Richter, R., Dennerlein, S., Lightowers, R.N., and Chrzanowska-Lightowers, Z.M. (2010). Hungry codons promote frameshifting in human mitochondrial ribosomes. *Science* *327*, 301.
- Tsuchihashi, Z., and Brown, P.O. (1992). Sequence requirements for efficient translational frameshifting in the *Escherichia coli* dnaX gene and the role of an unstable interaction between tRNA(Lys) and an AAG lysine codon. *Genes Dev.* *6*, 511–519.
- Weiss, R.B., and Gallant, J.A. (1986). Frameshift suppression in aminoacyl-tRNA limited cells. *Genetics* *112*, 727–739.
- Weiss, R.B., Dunn, D.M., Atkins, J.F., and Gesteland, R.F. (1987). Slippery runs, shifty stops, backward steps, and forward hops: -2, -1, +1, +2, +5, and +6 ribosomal frameshifting. *Cold Spring Harb. Symp. Quant. Biol.* *52*, 687–693.
- Yan, S., Wen, J.D., Bustamante, C., and Tinoco, I., Jr. (2015). Ribosome excursions during mRNA translocation mediate broad branching of frameshift pathways. *Cell* *160*, 870–881.
- Yelverton, E., Lindsley, D., Yamauchi, P., and Gallant, J.A. (1994). The function of a ribosomal frameshifting signal from human immunodeficiency virus-1 in *Escherichia coli*. *Mol. Microbiol.* *11*, 303–313.

STAR★METHODS

KEY RESOURCES TABLE

REAGENT or RESOURCE	SOURCE	IDENTIFIER
Bacterial and Virus Strains		
<i>E. coli</i> BL21(DE3)	Merck	69450
<i>E. coli</i> MRE 600 (1/2 log)	UAB Fermentation Facility	ATCC 29417 f
<i>E. coli</i> MDP_451	This paper	N/A
Biological Samples		
tRNA from <i>E. coli</i> MRE 600	Roche	10109550001
Chemicals, Peptides, and Recombinant Proteins		
AQUA peptides Ultimate grade RVNRQPLPARGR(+10) KRVRQPLPARGR(+10)	Thermo Fisher	N/A
3X FLAGPeptide	Sigma	F4799
LysC Protease	Roche	11047825001
Anti-FLAG M2 Magnetic Beads	Sigma	M8823
[³ H]Met	Perkin Elmer	NET061X
[¹⁴ C]Lys	HARTMANN ANALYTIC GmbH	ARC 0673
[¹⁴ C]Arg	HARTMANN ANALYTIC GmbH	MC 137
[¹⁴ C]Glu	Perkin Elmer	NEC290E
[¹⁴ C]Ser	HARTMANN ANALYTIC GmbH	MC 265
Phosphoenol pyruvate	Sigma	10108294001
Pyruvate kinase (PK)	Sigma	10109045001
Complete, EDTA-free	Roche	05056489001
Puromycin dihydrochloride	Sigma	P7255-250MG
B-PER reagent	Thermo Fisher	90079
Heptafluorobutyric acid (HFBA)	Sigma	52411-25ML-F
Oligonucleotides		
MDP_AMZ: GCGGTATTGGTAGTCCCACAACACCGTACCGTAACAAGCAGG CATACA	Eurofins Genomics	N/A
MDP_ANU: TTCGGGCTAAGACCTGATAACTCTTGTCGTCATCGTCTTTGT AGTCCATTGGCAGGCTCTGAAAC	Eurofins Genomics	N/A
MDP_ANT: GTTTCAGAGCCTGCCAATGGACTACAAAGACGATGACGACAAG AGTTATCAGGTCTTAGCCCGAA	Eurofins Genomics	N/A
MDP_ANA: CGTCTATTGAATCGGAGCACCCACAGTAGACCGCCTTTACC AAACATAG	Eurofins Genomics	N/A
MP527: ACTGTGGGTGCTCCGATTCAATAGACGGATCCTCTAGAGTCGACCGGAGA	Eurofins Genomics	N/A
MP528: TACGGTGTGTGGGACTACCAATACCGCGGCGCGATCCCCGGGTACCGA	Eurofins Genomics	N/A
MDP_AMX F: CCGTACAAGCAGGCATACA	Eurofins Genomics	N/A
MDP_AMY R: AGACCGCCTTTACCAACATAG	Eurofins Genomics	N/A
For mRNA constructs see Table S4 .	N/A	N/A
Recombinant DNA		
plasmid pKO3	Link et al., 1997	N/A
plasmid pET24a	Merck	BIO-69749-3

(Continued on next page)

Continued		
REAGENT or RESOURCE	SOURCE	IDENTIFIER
Software and Algorithms		
Micromath Scientist	Micromath	N/A
KinTek Explorer	KinTek Corporation	N/A
Skyline 3.6	https://skyline.ms/project/home/software/Skyline/begin.view	N/A
Other		
LiChrospher 100 RP-8 (5 μ m) LiChroCART 250-4	Merck	1.50832.0001
LiChrospher WP 300 (5 μ m) RP-18	Merck	1.50179.7116
Sepharose 4B gel filtration base matrix	GE Healthcare	17-0120-01
Phenyl Sepharose High Performance	GE Healthcare	17-1082-01
DEAE Toyopearl 650M	Tosoh Bioscience	07473
Reprosil-Pur 120 C18-AQ 5 μ m	Dr. Maisch GmbH	r15.aq
Reprosil-Pur 120 C18-AQ	Dr. Maisch GmbH	r119.aq
0.2 μ m SPARTAN syringe filter	GE Healthcare	514-1232

CONTACT FOR REAGENT AND RESOURCE SHARING

Further information and requests for resources and reagents should be directed to and will be fulfilled by the Lead Contact, Marina V. Rodnina (rodnina@mpibpc.mpg.de).

METHOD DETAILS

Introducing a FLAG tag

Chromosome-encoded *dnaX* gene from *E. coli* strain BL21(DE3) was tagged N-terminally with a FLAG-tag (coding for DYKDDDDK). The genomic regions on either side of the insertion were PCR amplified with primers MDP_AMZ and MDP_ANU, or MDP_ANT and MDP_ANA, and plasmid pKO3 (Link et al., 1997) was PCR amplified with primers MP527 and MP528. The three PCR products were assembled into a circular plasmid using Gibson Assembly (Gibson et al., 2009), and the genomic modification was generated by two-step homologous recombination. The insertions were verified by sequencing a 1325 base pair PCR product generated using primers MDP_AMX and MDP_AMY, using the same primers. The resulting strain is called MDP_451.

mRNA constructs

We used a variant of the original *dnaX* frameshifting site with the essential elements of frameshifting, the internal SD sequence, the SS and the SL, as in the wild-type sequence. The spacing between the stimulatory elements was also unchanged compared to the original *dnaX* frameshifting site. The K codon (AAA) two codons upstream of the slippery site was changed to AUG, which was used as the start codon. The codons following the slippery site AGU₁₀ and GAA₁₃ encoding for Ser and Glu, respectively, were mutated to UUC₁₀ and UAA₁₃, which encode for Phe and a stop, respectively, in the 0-frame. These replacements were introduced to simplify the separation and quantification of peptides by RP HPLC.

The mRNAs were prepared by *in-vitro* transcription using T7 RNA-polymerase and purified by fast protein liquid chromatography (FPLC). The mRNA constructs are listed in Table S4 (start codon is underlined, the slippery sequence and the stem loop are indicated by SS and SL, respectively).

tRNA preparation

tRNA^{fMet}, tRNA^{Ala}, tRNA^{Lys}, tRNA^{Arg}, tRNA^{Ser}, tRNA^{Glu}, tRNA^{Phe}, and tRNA^{Val} were prepared from total *E. coli* tRNA by consecutive column chromatographies on Sepharose 4B (GE Healthcare), Phenyl Sepharose (GE Healthcare), and DEAE Toyopearl 650M (Tosoh Bioscience). Aminoacylation of tRNAs with ¹⁴C-labeled or non-radioactive amino acids was performed according to established protocol (Kothe et al., 2006). Aminoacylated tRNAs were purified by reversed-phase HPLC on an LiChrospher WP 300 (5 μ m) RP-18 HPLC column (250 mm x 10.5 mm, Merck) equilibrated with buffer (20 mM ammonium acetate, pH 5.0, 10 mM magnesium acetate, 400 mM NaCl) using a gradient of 0%–15% ethanol. Aa-tRNAs were precipitated with ethanol and dissolved in water; concentrations were determined photometrically by absorbance at 260 nm.

Translation assays

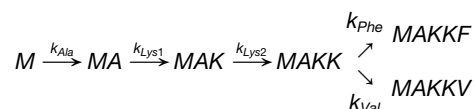
The experiments were carried out in buffer A (50 mM Tris-HCl [pH 7.5], 70 mM NH₄Cl, 30 mM KCl, 7 mM MgCl₂) supplemented with GTP (1 mM) at 37°C. Ribosomes from *E. coli* MRE 600, EF-Tu, EF-G, and initiation factors were prepared according to detailed

protocols (Cunha et al., 2013; Rodnina et al., 1997; Rodnina et al., 1999; Savelsbergh et al., 2003). To prepare initiation complexes, 70S ribosomes (1 μ M) were incubated with a 3–5-fold excess of mRNA, a 1.5-fold excess of f³H]Met-tRNA^{Met} and a 1.2-fold excess of IF1, IF2 and IF3 each in buffer A for 30 min. Initiation complexes were purified by centrifugation through a sucrose cushion (1.1 M) in buffer A. Ternary complexes were prepared by incubating EF-Tu (2-fold excess over aa-tRNA) together with GTP (1 mM), phosphoenolpyruvate (3 mM), and pyruvate kinase (0.1 mg/ml) in buffer A for 15 min and then with the purified aa-tRNAs for 1 min.

Translation experiments were performed in buffer A at 37°C either as end-point experiments (60 – 120 s incubation) by hand or using a KinTek RQF3 quench-flow apparatus. Translation experiments were carried out by rapidly mixing initiation complexes (0.2 μ M after mixing) with the respective ternary complexes as indicated (1 μ M) and EF-G (2 μ M) with GTP (1 mM). Reactions were quenched by the addition of KOH (0.5 M), and peptides were released by incubation for 30 min at 37°C. After neutralization with acetic acid, samples were analyzed by HPLC (LiChroSpher100 RP-8 HPLC column, Merck) using a gradient of acetonitrile in 0.1% heptafluorobutyric acid (HFBA).

The elution times of the reaction products were established using a set of model peptides synthesized in vitro: f³H]Met[¹⁴C]Ala, f³H]MetAla[¹⁴C]Lys, f³H]MetAla[¹⁴C]Arg, f³H]MetAla[¹⁴C]Lys[¹⁴C]Lys, f³H]MetAla[¹⁴C]ArgLys, f³H]MetAla[¹⁴C]Lys[¹⁴C]LysPhe, or f³H]MetAla[¹⁴C]Lys[¹⁴C]LysVal. The extent of product formation was determined from the ratio of f³H]Met in the respective peak to the total ³H-radioactivity in the eluate. Quantification of f³H]MetAlaLysLys[¹⁴C]Ser and f³H]MetAlaLys[¹⁴C]GluVal was based on the amount of [¹⁴C]Ser or [¹⁴C]Glu radioactivity in peptides. The frameshifting efficiency (–1FS) was calculated from the end points of in vitro translation experiments; the values are mean \pm s.d. (n = 3 or more independent experiments).

Time courses were evaluated by numerical integration using Micromath Scientist and KinTek Explorer software according to the following model:



where k_{Ala} , k_{Lys1} , k_{Lys2} , k_{Phe} and k_{Val} are rate constants of the incorporation of the respective amino acid into the peptide. An analogous model was used to evaluate peptide synthesis in the presence and absence of Arg-tRNA^{Arg}. The fraction of non-progressing ribosomes was taken into account by drop-off parameters in the model. Standard deviations of rates (Tables S1 and S2) were determined by numerical integration using in-built software routines assuming 95% confidence limit. All kinetic experiments were repeated at least twice.

Mass Spectrometry

Chromosome-encoded *dnaX* gene from *E. coli* strain BL21(DE3) was tagged N-terminally with a FLAG-tag (coding for DYKDDDDK) using two-step homologous recombination (Link et al., 1997). Cells were grown to a density of 1.8 OD₆₀₀ in 500 mL Lysogeny Broth (LB) medium cultures in baffled flasks at 37°C. Cells were lysed using B-PER reagent (ThermoFisher Scientific) in 25 mM HEPES pH 7.5, 200 mM KCl, 10 mM MgCl₂, supplemented with complete protease inhibitor (Roche), DNase, puromycin (100 μ M), and lysozyme (trace amounts). The lysate was cleared by centrifugation (30 min, 108,800 x g, 4°C) and filtration (0.2 μ m SPARTAN syringe filter (GE Healthcare)). Tagged DnaX was isolated by immunoprecipitation using anti-FLAG M2 magnetic beads (SIGMA) and eluted with 3X FLAG peptide (SIGMA) according to the manufacturer's protocol.

To express the isostoichiometric reference protein from a plasmid, the chromosome-encoded *dnaX* gene was amplified from BL21(DE3) and cloned into pET24a (Novagen) using BamHI/XhoI. Two nucleotides necessary to establish the –2-frame product were introduced by PCR. The protein was expressed in BL21(DE3) after induction with IPTG (1 mM) for 1.5 hr in LB medium as described above. Cells (0.1 OD₆₀₀) were lysed in Laemmli buffer (BIORAD) and proteins were separated on a 15% SDS-PAGE.

To remove the excess of the FLAG peptide used for elution (see above) and to reduce the sample complexity, proteins were separated by SDS-PAGE. The band corresponding to *dnaX* –1 and –2 frameshifting products were excised and in-gel proteolysis was performed as described (Shevchenko et al., 2006) with minor modifications. Briefly, proteins were reduced with 10 mM DTT for 45 min at 56°C and then alkylated with 55 mM iodoacetamide in 50 mM ammonium bicarbonate for 20 min at 23°C in the dark. Protein digestion was performed overnight at 37°C at a 1:100 (w/w) LysC (Roche) to protein ratio. Following digestion, peptides were extracted from the gel and concentrated by vacuum evaporation to dryness. Peptides were dissolved in 25 μ l of 5% (v/v) trifluoroacetic acid/2% (v/v) acetonitrile.

DnaX peptides were analyzed by RP HPLC–electrospray ionization–tandem mass spectrometry using a Dionex Ultimate 3000 HPLC system connected to a QExactive Plus mass spectrometer (Thermo Scientific). First, extracted peptides (100–300 fmol) were loaded onto an in-house packed C18 ‘trapping’ column (0.1 μ m x 20 mm, Reprosil-Pur 120 C18-AQ 5 μ m) connected in tandem with a C18 column (an analytical C18 capillary column; 0.075 mm x 280 mm column packed with 1.9 μ m Reprosil-Pur 120 C18-AQ). Peptides were eluted using a 50 min linear gradient of 2.5–35% acetonitrile in 0.1% formic acid at 300 nl/min. The instrument was operated in targeted acquisition mode analyzing the precursor and fragment ions of the most prominent charge state by scheduled selected ion monitoring (tSIM) and parallel reaction monitoring (PRM), respectively (Gallien et al., 2012; Peterson et al., 2012). For tSIM the resolution was 70,000, the AGC target was 1x 10⁶, the maximum fill time was 100 ms, and the isolation window was 4 m/z. For PRM the resolution was 70,000, the AGC target 5x10⁶, and the maximum fill time was 300 ms. Ions were isolated within

a 0.7 m/z isolation window and fragmented with HCD collision energy 28 eV. The elution windows (4 min) of all peptides were scheduled. Elution profiles of precursor ions (tSIM) and fragments (PRM) were extracted and integrated in Skyline (MacLean et al., 2010) at a resolution of 70,000 (Figure S3).

The -2-frame peptide selected for quantification was the only peptide in the sequence amenable for such analysis. The peptide is proteotypic because it does not occur in the 0-frame proteome of *E. coli* BL21(DE3). However, it is not an optimal quantotypic peptide, because it is hydrophilic and highly charged and thus elutes early in RP HPLC runs. It has two residues that can be deamidated (< 10% as estimated by label-free quantification) and two neighboring basic amino acids at the N terminus potentially rendering it sensitive to higher rates of missed cleavages (< 10% as quantified by absolute quantification of the fully processed and missed-cleaved product using AQUA peptides, stable isotope-labeled peptides comprising $^{13}\text{C}_6$ $^{15}\text{N}_4$ at the C-terminal Arg of high purity and concentration accuracy ($\pm 5\%$)). For quantification, the sum of the ions at the MS1 or MS2 level was individually considered. In order to determine the frameshifting efficiency the integrated areas were normalized to correct for differences in peptide hydrophobicity, ionizability, chemical stability or enzymatic digestion efficiency by corrective response factors. The response factors were established using an overexpressed *dnaX* construct in which the three shared peptides and the -2 frame peptide had a 1:1:1:1 stoichiometry. The response factors of the 12 replicates (four biological and three technical each) were averaged to generate one response factor per reference peptide. The chromosome-encoded DnaX was analyzed in four biological replicates with three technical replicates each (Table S3). The integrated areas for the -2-frame peptide were normalized by the three averaged response factors for each reference peptide to calculate the frameshifting efficiency per reference peptide and replicate. Altogether, 36 individual frameshifting efficiencies were calculated and averaged. The frameshifting efficiencies were measured in the linear dynamic range of the mass spectrometer and were independent of the amount of proteolyzed DnaX loaded onto the column (data not shown).

Molecular Cell, Volume 66

Supplemental Information

Conditional Switch between Frameshifting

Regimes upon Translation of *dnaX* mRNA

Neva Caliskan, Ingo Wohlgemuth, Natalia Korniy, Michael Pearson, Frank Peske, and Marina V. Rodnina

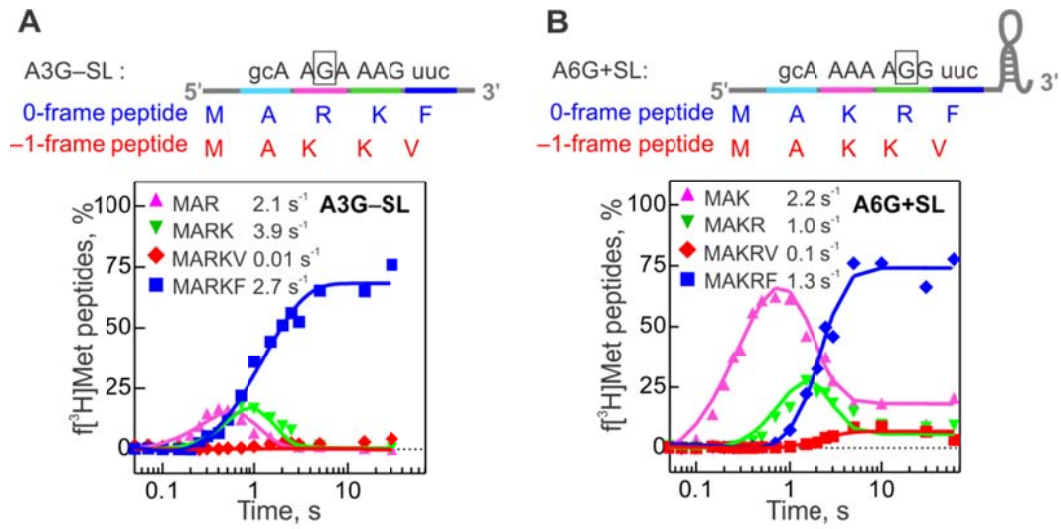


Figure S1. Kinetics in the presence of the cognate Arg-tRNA^{Arg}. Related to Figures 2 and 3.

(A) A3G-SL mRNA.

(B) A6G+SL mRNA. MAR (pink), MARK (green), MARKF (blue) and MARKV (red) peptides are monitored.

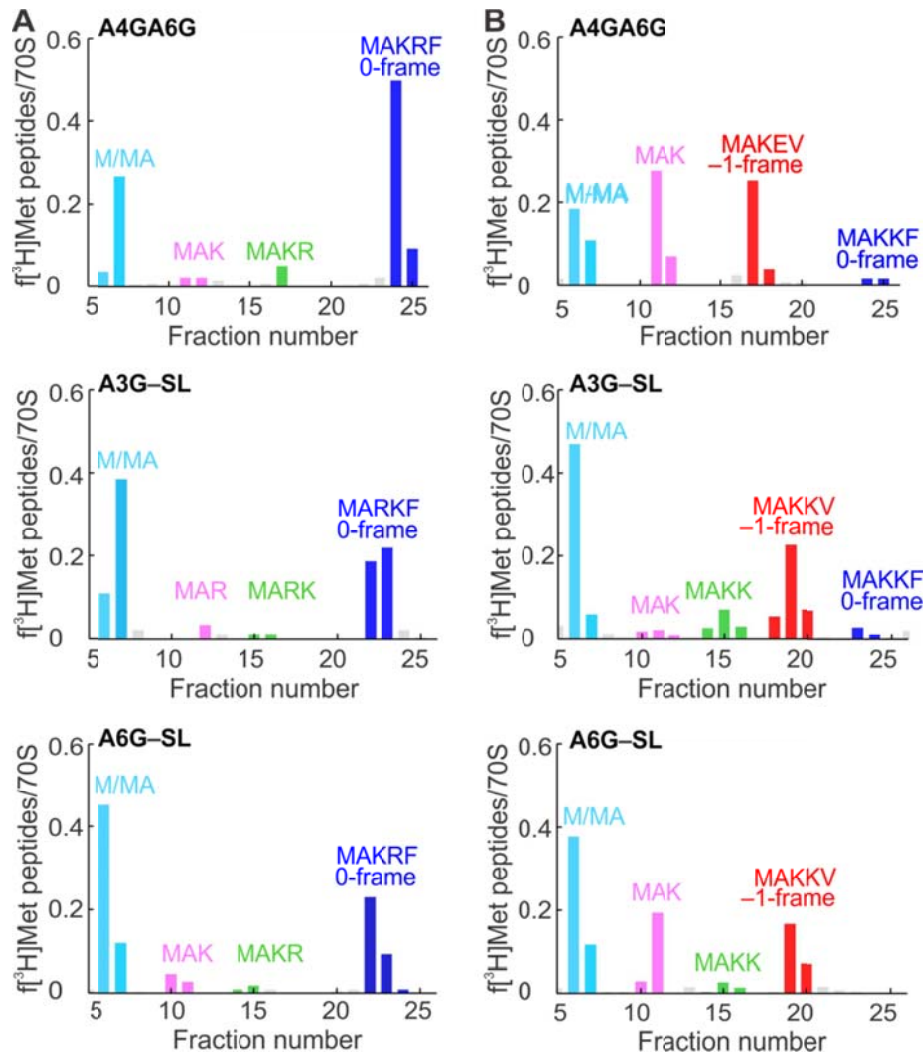


Figure S2. Analysis of translation peptides. Related to Figures 2, 3 and 4.

(A) Example chromatograms for peptide synthesis on the A4GA6G (top), A3G-SL (middle panel) and A6G-SL mRNA variants in the presence of Arg-tRNA^{Arg}. Monitored peptides are M-MA (light blue), MAK or MAR (pink), MAKR or MARK (green), and MAKRF or MARKF (blue).

(B) Same as in **(A)**, but without Arg-tRNA^{Arg}. Monitored peptides are M-MA (light blue), MAK (pink), MAKK (green), MAKEV-MAKKV (red) and MAKKF (blue).

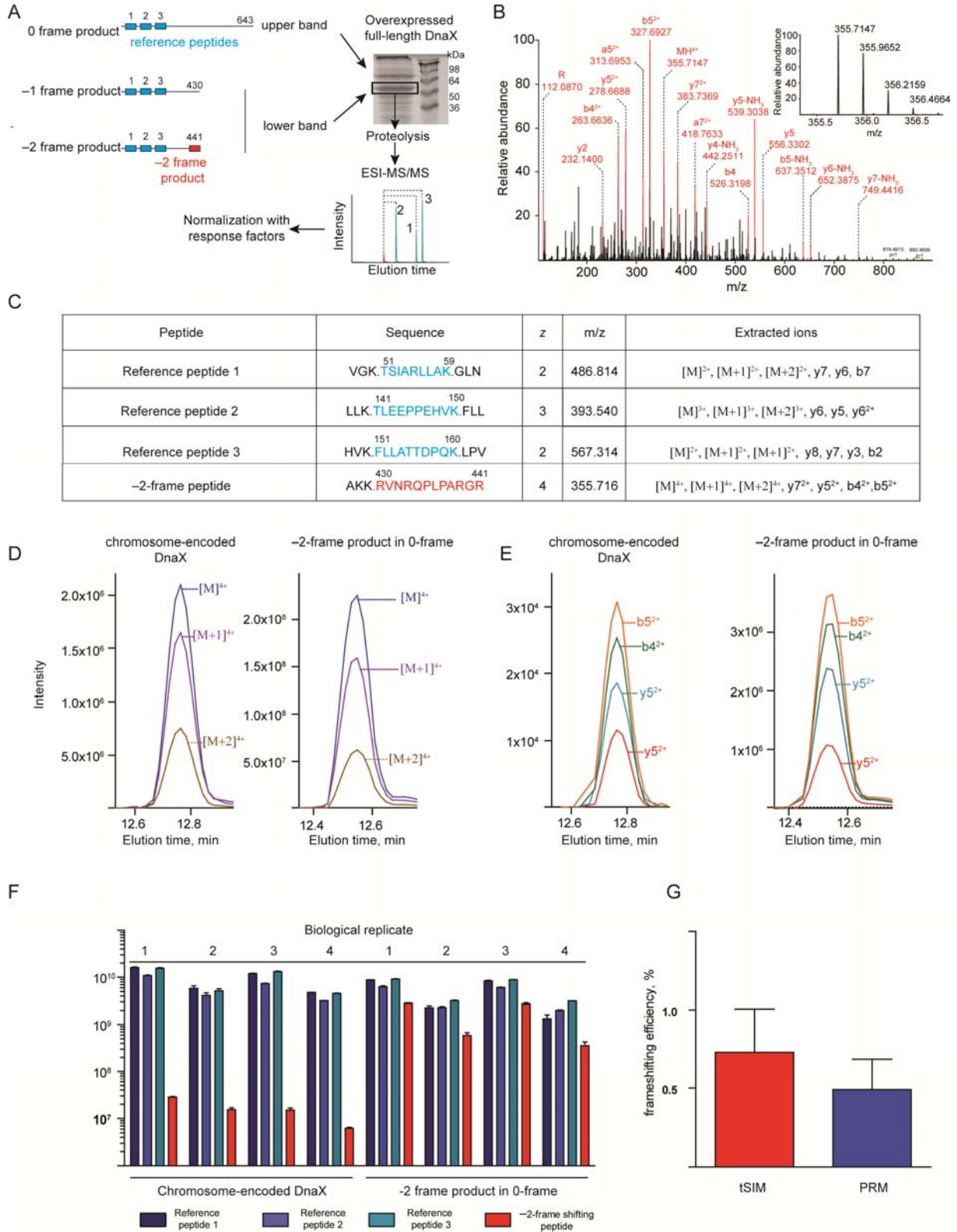


Figure S3. Quantification of -2-frame product of *dnaX* translation *in vivo* using mass spectrometry. Related to Figure 5. See also Table S3.

(A) Quantification work flow. The -2-frame product was quantified relative to the -1-frame product. The two products have a similar size and co-migrate on SDS PAGE. The protein band that comprised both isoforms was excised from the gel and subjected to proteolysis with LysC. The amount of -2-frame relative to -1-frame product was quantified by label-free targeted mass spectrometry monitoring the elution of precursor- (targeted selected ion monitoring; tSIM) and fragment- (Parallel Reaction Monitoring; PRM) ions over time.

(B) The -2-frame peptide identified by high resolution MS (inset, isotope dot product 0.99) and MS/MS spectra as well as by co-elution and co-fragmentation with an isotope-labeled internal standard peptide (AQUA, ratio dot product 0.99).

(C) Sequence and extracted ions of the quantified peptides.

(D) Representative elution profiles of the -2-frame peptide precursors ions (tSIM).

(E) Representative elution profiles of the -2-frame peptide fragment ions (PRM).

(F) Integrated areas for the -2-frame peptide and the three reference peptides (shown for PRM) (**Table S3**). For both samples four biological replicates were analyzed. Error bars show the standard deviation of three technical replicates.

(G) Efficiency of -2- relative to -1-frameshifting. The frameshifting efficiency was independently quantified on MS1 (0.7%; red tSIM) and MS2 (0.5%; red; PRM) level. Error bars represent the SD of four biological replicates with three technical replicates each.

Table S1. Rate constants of translation steps upon –1PRF on *dnaX*. Related to Figure 1.

mRNA variant	Rates, s ⁻¹				–1FS, %	
	LysI ^a	LysII ^a	Val ^a	Phe ^a	QF	IVT
SS / SL	1.7±0.2	2.0±0.2	0.46±0.03	0.13±0.02	78±15	72±4
– / SL	2.1±0.3	1.3±0.1	0.03±0.01	0.3±0.0	9±3	4±1
SS / –	2.3±0.5	2.2±0.1	0.7±0.03	2.3±0.1	23±2	16±5
– / –	2.3±0.5	2.2±0.5	0.03±0.01	2.9±0.6	1±0	0

^a Rate constants of amino acid incorporation were determined by global fitting of the data shown in Figures 1E-1H; error bars are s.e.m. of the fit. IVT, *in-vitro* translation. The frameshifting efficiency (–1FS) was calculated from the end points of IVT experiments shown in Figures 1C and 1D; the values are mean ± s.d. (n=3 independent experiments).

Table S2. Rate constants of translation steps upon NHF on various *dnaX* constructs. Related to Figures 2, 3 and 4.

mRNA variant	Rates, s ⁻¹		–1FS, %
	Lys ^a	Val ^a	IVT
A3G+SL	n.d.	0.06±0.01	80±4
A3G–SL	n.d.	0.04±0.02	61±4
A6G+SL	2.3±0.1	0.03±0.00	52±8
A6G–SL	2.4±0.1	0.02±0.00	44±4
A4GA6G	1.4±0.1	0.014±0.002	36±4

^a Rates constants of amino acid incorporation were determined by global fitting of the data shown in Figures 2F, 2G, 3F, 3G and 4D; error bars are s.e.m. of the fit. The frameshifting efficiency (–1FS) was calculated from the end points of IVT experiments shown in Figures 2D, 2E, 3D, 3E, and 4C; the values are mean ± s.d. (n=3 independent experiments).

Table S3. Determination of the -2 frameshifting efficiency by mass spectrometry *in vivo*. Related to Figure 5 and S3.

This table is a separate file.

Table S4. mRNA constructs used in this study. Related to Star Methods.

REAGENT or RESOURCE	SOURCE	IDENTIFIER
Oligonucleotides		
SS / SL mRNA: GCGUGCAGGGAGCAACCAUGGCAAAAAAGUUC UAACCGGCAGCCGCUACCCGCGCGCGGCCGGU GAA	This paper	N/A
- / SL mRNA: GCGUGCAGGGAGCAACCAUGGCGAAGAAGUUC UAACCGGCAGCCGCUACCCGCGCGCGGCCGGU GAA	This paper	N/A
SS / - mRNA: GCGUGCAGGGAGCAACCAUGGCAAAAAAGUUC UAG	This paper	N/A
- / - mRNA: GCGUGCAGGGAGCAACCAUGGCGAAGAAGUUC UAG	This paper	N/A
A3G-SL mRNA: GCGUGCAGGGAGCAACCAUGGCAAGAAAGUUC UAG	This paper	N/A
A3G+SL mRNA: GCGUGCAGGGAGCAACCAUGGCAAGAAAGUUC UAACCGGCAGCCGCUACCCGCGCGCGGCCGGU GAA	This paper	N/A
A6G-SL mRNA: GCGUGCAGGGAGCAACCAUGGCAAAAAGGUUC UAG	This paper	N/A
A6G+SL mRNA: GCGUGCAGGGAGCAACCAUGGCAAAAAGGUUC UAACCGGCAGCCGCUACCCGCGCGCGGCCGGU GAA-	This paper	N/A
A4GA6G mRNA: GCGUGCAGGGAGCAACCAUGGCAAGAGGUUC UAACCGGCAGCCGCUACCCGCGCGCGGCCGGU GAA	This paper	N/A